

PRIMARY ACCELERATION MEASUREMENT USING FRINGE COUNTING WITH HETERODYNE INTERFEROMETRY

Dr. Thomas Bruns, Frank Blume, Henrik Volkers

¹*Physikalisch Technische Bundesanstalt (PTB), Braunschweig, Germany, thomas.bruns@ptb.de*

Abstract: The application of heterodyne interferometry with direct access to the frequency modulated signal was deemed unfeasible for low frequency vibration measurement, because of the trade-off between a carrier frequency and modulation bandwidth in the MHz range calling for high sampling rates on the one hand, and the low vibration frequency calling for long measuring times on the other hand. Data acquisition systems with the necessary amount of sample memory are expensive and the CPU time needed for the appropriate data processing becomes prohibitive at very low vibration frequencies.

PTB recently developed a new method related to the classic homodyne fringe counting, which reduces the sampling rates for the interferometer signal to ranges related to the spectral contents of the vibration motion.

The new method of heterodyne fringe counting is capable of magnitude and phase response measurements. The contribution describes the methodology and discusses some of its distinctive features and possible pitfalls.

Keywords: heterodyne Laser interferometry, primary accelerometer calibration, fringe counting

1. Introduction

The photodiode output of a heterodyne Laser vibrometer as used at PTB can mathematically be approximated for sinusoidal excitation by:

$$I(t) = I_0 \sin\left(2\pi\left(f_c \cdot t + \frac{2 \cdot s(t)}{\lambda}\right)\right), \quad (1)$$

with an amplitude $I_0 \approx 0,2 \text{ V}$, a carrier frequency $f_c \approx 40 \text{ MHz}$, the He-Ne laser wavelength $\lambda = 633 \text{ nm}$, and $s(t) = s_0 \cdot \sin(\omega_v t - \varphi_v)$ being the vibration displacement.

In former publications the direct use of the signal was implemented either by using time interval analysers [1] or high speed ADCs [2]. The former are VXI-based devices that measure the time interval between subsequent zero crossings of the input signal with pico second accuracy, and as such provide an accurate estimate of the momentary frequency, however, these kind of devices vanished from the market and are no longer supplied. The implementation using high speed ADCs needs to sample the FM signal in compliance with the Nyquist condition, which leads to sampling rates of 200 MS/s and higher. Such sampling rates combined with the long data acquisition time of low

frequency vibration measurements are still prohibitive in terms of memory usage and signal processing time.

2. THE NEW METHODE

The argument of the sine function in (1) describes a generally increasing optical phase value:

$$\varphi_{\text{opt}} = 2\pi\left(f_c \cdot t + \frac{2s_0}{\lambda} \cdot \sin(\omega_v t - \varphi_v)\right) \quad (2)$$

A counter device triggered by the rising edge of a signal like (1) will, accordingly, provide a sequence of integers of the form

$$N(t) = \text{floor}\left(f_c \cdot t + \frac{2s_0}{\lambda} \cdot \sin(\omega_v t - \varphi_v)\right). \quad (3)$$

where floor(x) returns the nearest integer smaller or equal to x.

This counter signal, if sampled at appropriate time intervals, can be analysed with the classical sine approximation [3] provided the model equation is extended by a linear term.

That is, the function

$$\hat{N}(t) = a \cdot \sin(\omega_v t) + b \cdot \cos(\omega_v t) + f_c \cdot t + c \quad (4)$$

can be applied to fit the time series of counter results $N_i = N(t_i)$, with (a, b, c, f_c) being the fitted parameters. Figure 1 provides an impression of the vibration signal and a related counter signal.

With the relations

$$s_0 = \frac{\lambda}{2} \cdot \sqrt{a^2 + b^2} \quad (5)$$

and

$$\varphi_v = \tan^{-1}\left(\frac{b}{a}\right) \quad (6)$$

the essential vibration parameters can be calculated in accordance to ISO 16063-11 [3]. Hence, if the electrical output of the sensor under test is synchronously sampled, a calibration of the complex sensitivity in magnitude and phase is feasible.

As this process makes use of fringe counting, in a sense, the question arises, where the limits of the method in terms of resolution with reference to the displacement amplitude s_0 or the sampling rate are. Furthermore, disturbing components like noise, drift, distortion or jitter will be investigated. The subsequent sections of this paper will deal with these questions based on a simulation example.

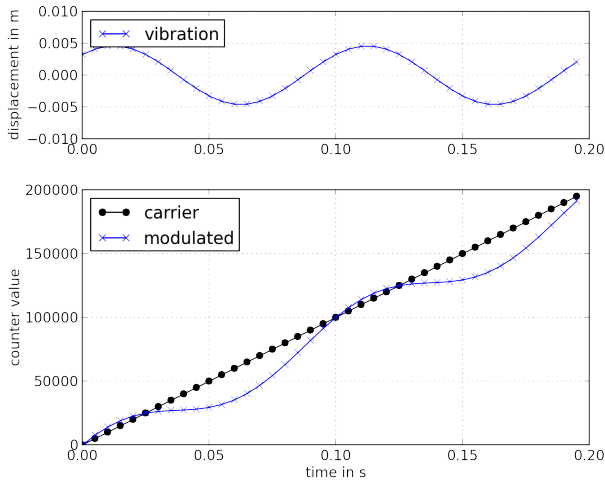


Fig. 1 Example of vibration movement time series (top) and the corresponding counter output

3. ACHIEVABLE RESOLUTION

As described above, the proposed methodology is based on fringe counting. In contrast to the homodyne fringe counting, where the total number of fringes per vibration period is the relevant figure, the sampling of a time series of counter values during vibration provides additional information. From Figure 2 it can be deduced that the instances, when the counter increases its value due to a new fringe, carry essential information about the signal shape in terms of amplitude and phase.

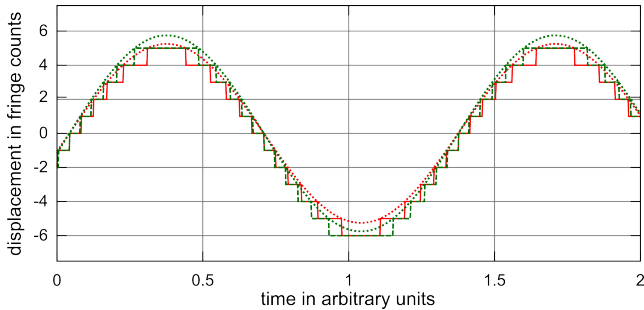


Fig. 2 Two sinusoidal signals of $\frac{1}{2}$ fringe difference in amplitude, together with their counter representation.

With the He-Ne laser typically used, the applied wavelength λ is 633 nm. Especially at higher frequencies and the respective small displacements this may be considered the limiting factor for the applicability of the method. Therefore, the case of 80 Hz vibration frequency was investigated as an example. With a sinusoidal acceleration amplitude of 1 m/s^2 to 10 m/s^2 at a vibration frequency of 80 Hz, the nominal displacement is between $4 \mu\text{m}$ and $40 \mu\text{m}$ or 6.3 to 63 fringes. Figure 3 shows the relative deviation between the nominal amplitude and the derived amplitude according to the evaluation of the counter time series.

The deviation decreases for increased amplitude as well as for increased sampling rate. Although the charted relative deviation exhibits a seemingly erratic behaviour, it is a

displacement dependent systematic effect, and its dispersion around a zero mean can be utilized to reduce the effect by averaging a set of measurements at slightly different amplitudes.

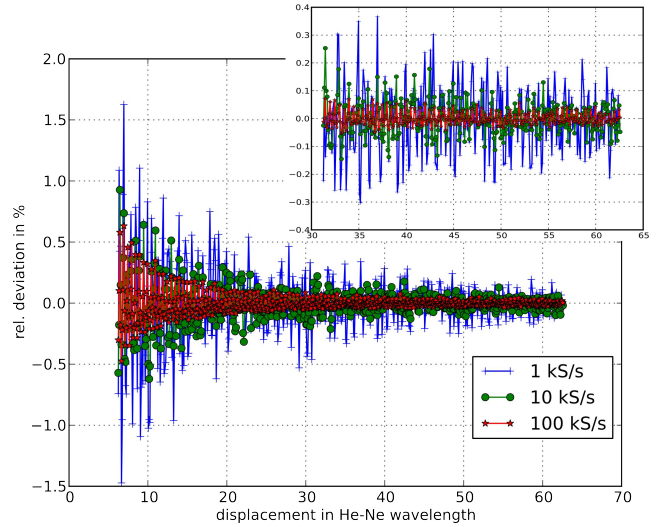


Fig. 3 Relative deviation of the fitted displacement amplitude to the nominal amplitude for different sampling rates

For 100 kS/s and 5 m/s^2 (30 fringes) vibration amplitude the relative deviation is well below 0.1% .

Averaging 20 measurements with normally distributed amplitudes of a standard deviation of 1.5λ further reduces the spread of the fitted results by a factor of 5 . In terms of an absolute amplitude resolution, this is a value well below one-hundredth of a wavelength.

The achievable resolution in dependence of the excitation frequency was investigated by Monte Carlo simulation (MC) in the range from 0.01 Hz to 100 Hz . For each frequency, a set of 5000 trials using the already described analysis method was computed. Each trial simulated a pure sine vibration with random initial phase and an amplitude $s_0 + \epsilon$, where s_0 is the minimum of the displacement at 10 m/s^2 acceleration or maximum stroke length and ϵ is a normal distributed random variation with a standard deviation of 1.5λ . The evaluation of the MC considered the deviation Δs of the fitted amplitude s to the given amplitude $s_0 + \epsilon$.

The mean of Δs over the 5000 runs is an estimator of a systematic uncertainty component (bias), while the standard deviation is an indicator of the repeatability of the method. These results are given relative to the input amplitude in Fig. 4.

4. PTB IMPLEMENTATION

While in the previous section the performance of the new method for a pure sine vibration was discussed, the implementation in a calibration set-up has to deal with various kinds of disturbances. In order to estimate the performance for a real implementation, several details of the measurement procedure and of the signal quality have to be considered. This will subsequently be done by making use of MC. The base for this simulation is the implemented

measurement procedure. Here, the following procedure is presumed and simulated accordingly:

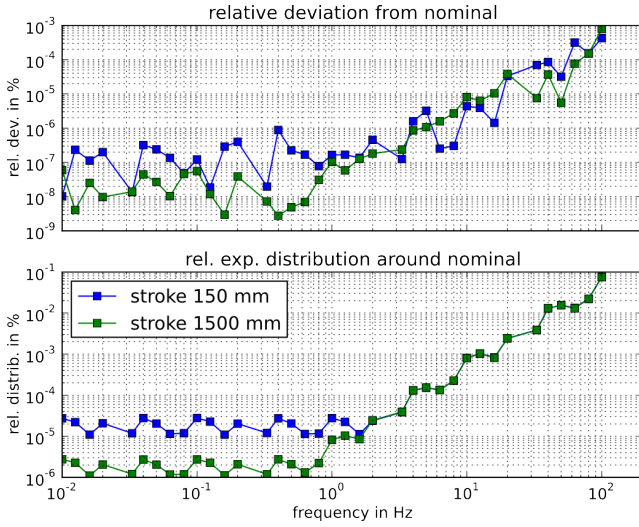


Fig.4 MC resolution investigation: results for the mean fit deviation Δs (top) and its standard deviation (bottom).

The vibration oscillation measured by laser interferometry has a nominal displacement amplitude of s_0 at the nominal frequency of f_0 . The sampling process starts when the oscillation has an arbitrary initial phase of $\varphi_{i,0}$. From this moment N consecutive periods of the nominal vibration will be sampled with a sampling rate of f_s .

Furthermore, the subsequently listed disturbing components are introduced in order to simulate a realistic impression of the capabilities of the method:

- zero drift of the vibration displacement (l_0)
- amplitude deviation (l_1) in terms of a positive or negative drift (e.g. due to heating of the shaker coil).
- harmonic distortion of the signal (h_3, h_5).
- jitter in terms of a random counter error

The analytical form of the applied displacement equation used in the calculation was:

$$s(t) = s_0 \cdot \left(1 + \frac{l_1}{\tau} \cdot t\right) \sum_{i=1}^5 h_i \cdot \sin(i\omega_0 t + \varphi_0) + \frac{s_0 \cdot l_0}{\tau} \cdot t \quad (7)$$

with τ being the data acquisition interval. The following standard deviations for the normal distributed parameters of the disturbances were applied:

Zero drift	$\sigma(l_0) = 0.03 = 3\%$
Amplitude drift	$\sigma(l_1) = 0.03 = 3\%$
Harmonic distortion	$\sigma(h_1) = 0$,
(of displacement)	$\sigma(h_3) = 0.33\%$,
	$\sigma(h_5) = 0.016\%$
Jitter	$\sigma_{\text{jitter}} = 1.5$ counts

Because some of these components generate a large deviation in relation to the nominal signal but cancel to

some extent when the magnitude of the complex sensitivity is calculated, a virtual sensor was implemented in software applying a nominal sensitivity of $1.0 \text{ V}/(\text{m}/\text{s}^2)$ and subjected to an acceleration input derived from the respective analytical displacement signal (7) as second derivative

$$a(t) = \frac{d^2}{dt^2} s(t) \quad (8)$$

To the calculated voltage signal a normal distributed random noise component of 8 mV was added, which is typical for one of the labs reference transducers.

The measurement procedure implemented at PTB samples a complete time series of a signal consisting of several periods of vibration. For the subsequent analysis, this series is dissected in single period intervals, which in turn are submitted to the sine fitting algorithm. Prior to the dissection, however, the influence of the carrier frequency is reduced by fitting a straight line to the counter data and subtracting this fit from the respective sampled values of the time series. After this detrending, a residual slope may still be detectable in the signal. This is considered by the subsequent sine approximation (SA) applied to the separate periods of the signal. Figure 5 visualizes the two steps of detrending and dissection.

For each of the N periods, the SA results in a set of coefficients, namely (a, b) for the magnitude of vibration, c for the offset and d for the residual slope.

For the measured mean of magnitude \hat{s} and phase $\hat{\varphi}$ of the complete time series the following averaging is applied:

$$\hat{s} = \frac{\lambda}{2 \cdot N} \cdot \sqrt{\left(\sum a_i\right)^2 + \left(\sum b_i\right)^2} \quad (9)$$

$$\hat{\varphi}_{i,0} = \tan^{-1} \left(\frac{\sum b_i}{\sum a_i} \right) \quad (10)$$

Finally, for the selection of measurement parameters the ranges given in Table 1 were distinguished.

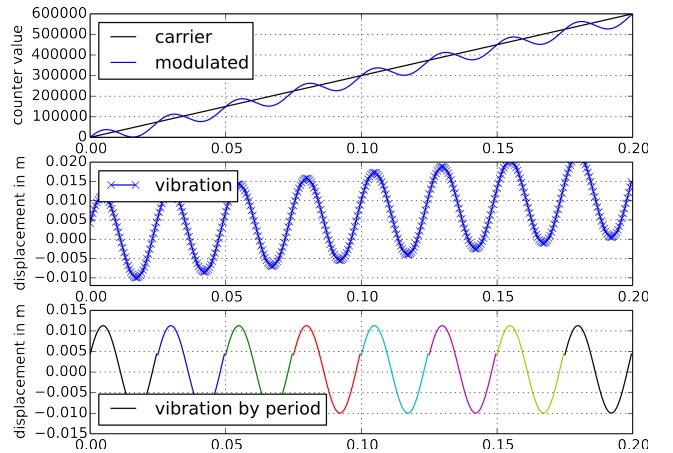


Fig. 5 Exaggerated pictorial description of the applied signal processing steps: Counter time series (top), detrended counter time series (centre), dissected sine approximation of the sampled series (bottom).

Table 1: data acquisition parameters for the MC

f_s in S/s	N	f_0 in Hz
5	80	0,01
10	60; 80	0,0125; 0,016
20	50; 70; 80	0,02; 0,033; 0,04
50	50; 60; 70; 80	0,05; 0,063; 0,08; 0,1
100	60; 80	0,125; 0,16
...
50 000	50; 60; 70; 80	50; 63, 80, 100

The results are depicted in Figure 6. The error bars (scaled to arbitrary units) in the lower two charts for acceleration and voltage indicate the variability of the MC trials, which increases with decreasing displacement amplitude, i.e. increasing frequency.

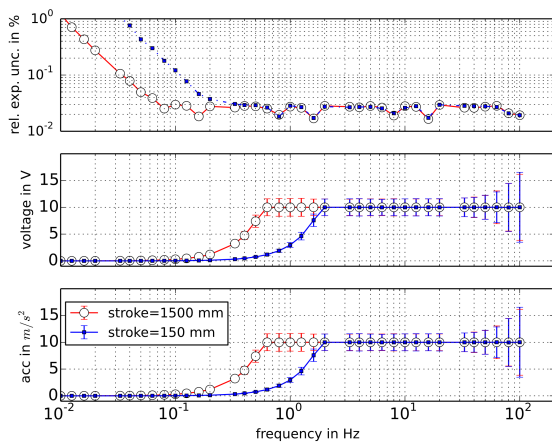


Fig. 6 Results of the MC simulation with error bars indicating the spread of the MC trials, acceleration (bottom), sensor voltage (centre) and the relative expanded deviation from nominal sensitivity (top)

From the top chart, which represents the relative deviation from the nominal value of the magnitude of sensitivity, it is evident, that the resolution of the method is excellent in the given frequency range. Although the dispersion of acceleration and voltage increase for high frequencies, the relative expanded deviation stays (almost) constant for frequencies beyond 0.3 Hz. For lower frequencies, the relative deviation increases due to the decrease in signal-to-noise ratio with decreasing sensor voltage.

5. Summary and Conclusion

A new efficient method for the acquisition and analysis of heterodyne laser vibrometer signals was described in this contribution. The method allows for a reasonable choice of the sampling rate in relation to the applied vibration frequency for the frequency modulated heterodyne signal. This makes it especially suitable for low frequency primary vibration calibration.

6. REFERENCES

- [1] W Wabinski; H.-J. v. Martens, "Time interval analysis of interferometer signals for measuring amplitude and phase of vibrations", Proc. SPIE, Vol. 2868, p. 166-177, 1996
- [2] Th. Bruns, M. Kobusch, "Data Acquisition and Processing for PTB's Impact Force Standard Machine", Proc. of IMEKO TC3 Conference, Cairo, Egypt, 2005
- [3] ISO 16063-11:1999 Methods for the calibration of vibration and shock transducers -- Part 11: Primary vibration calibration by laser interferometry